

tude, the ASE has a shape resembling that from erbium doped fibre amplifiers. The signal intensity at the output of the waveguide is plotted in Fig. 3 as a function of the pump power at the output of the coupler. We see from Fig. 3 that the light

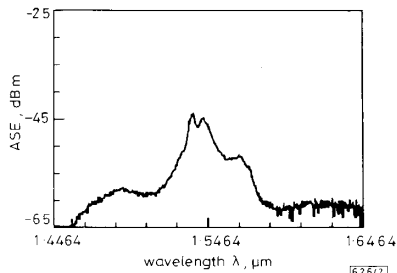


Fig. 2 ASE spectrum recorded in 2.4 cm long  $Er^{3+}$ -doped sodium calcium silicate glass waveguide

Waveguide width is  $6 \mu m$  and its thickness is  $(1.3 \pm 0.1) \mu m$   
Pump power is 120 mW at 975 nm  
Resolution window of spectrum analyser is 0.5 nm

output went from a loss of 21 dB at zero pump power to a gain/loss of 0 dB at a pump power of 120 mW. Therefore the power required for transparency of the guide is probably  $\sim 60$  mW (assuming 3 dB coupling loss at 975 nm). A clear change in slope of the gain against power curve is observed in Fig. 3 at  $\sim 20$  mW. We think that this saturation is associated with upconversion of the pump radiation. A bright green light emitted from the pumped waveguide is clearly visible.

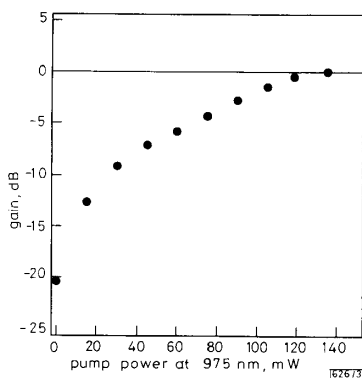


Fig. 3 Measured gain pump power for 2.4 cm long  $Er^{3+}$ -doped sodium calcium silicate glass waveguide described in text

3 dB correction in signal intensity compensating for estimated coupling loss is incorporated in results

We believe that this observed 21 dB enhancement in light output on pumping shows that significant levels of stimulated emission could be excited in the doped waveguide. This is promising for the realisation of an ultrashort length integrated amplifier on silicon.

6th April 1992

J. Shmlovich, Y. H. Wong, P. C. Becker, A. J. Bruce and R. Adar (AT&T Bell Laboratories, Murray Hill, New Jersey 07974-0636, USA)

A. Wong (Massachusetts Institute of Technology, Cambridge, Massachusetts 02139, USA)

#### References

- SHMULOVICH, J., WONG, A., WONG, Y. H., BRUCE, A. J., BECKER, P. C., GRODKIEWICZ, W. H., and BERKSTRESSER, G. W.: 'Deposition and characterization of Er-doped silicate films on silicon', *Ceramic Trans.*, Solid State Optical Materials, American Ceramic Society, 1992

- HENRY, C. H., and VERBEEK, B. H.: 'Solution of the scalar wave equation for arbitrarily shaped dielectric waveguides by two-dimensional Fourier analysis', *J. Lightwave Technol.*, 1989, LT-7, (2), pp. 308-313

## EFFECTS OF ANTENNA SECTORISATION ON DATA RATE LIMITATIONS OF INDOOR RADIO MODEMS

G. Yang, K. Pahlavan and T. Holt

Indexing terms: Radiocommunication, Local area networks

A deterministic model of indoor radio propagation that uses ray tracing techniques is introduced. This model is suitable for analysing the performance of sector antenna systems in an indoor radio environment. Using this model, the effects of sectorisation of the antenna on the data rate limitations of BPSK and BPSK/DFE modems operating in an indoor radio channel are analysed.

**Introduction:** Wireless local area networks (WLLANs) demand high data rates, but the maximum data rate in indoor radio channels is bounded due to the effects of multipath. To increase the data rate, performance enhancement techniques such as external diversity, coding, adaptive equalisation, and spread spectrum have been studied.

This Letter presents an analytical approach to examine the effectiveness of sector antennas [1] in increasing the data rate limitations of BPSK and BPSK/DFE modems operating in the indoor radio environment. A sector antenna observes the signal arriving from different directions (paths) and selects the one with maximum power. Because the signals are arriving from different directions, the sector antenna potentially reduces the effects of multipath, resulting in a higher attainable data rate for the radio modem.

For a realistic performance evaluation of the modems, the measured channel profiles are usually used [2] to represent the channel in the calculation of the error rates. However, all of the available channel measurements have been performed with omnidirectional antennas and therefore the direction from which the paths arrive is not specified. As a result, they cannot be used for performance evaluation of systems with sector antennas. To analyse the performance of these systems, a new channel model which provides the directions of arriving paths in indoor radio channels is required.

**Channel model:** A deterministic model using ray tracing techniques is used to model the radio channel [3, 4]. This model provides, in addition to the magnitude, phase and delay of each path, the direction of the arriving signal path. This makes it suitable for the performance evaluation of systems using sector antennas. The ray tracing algorithm is useful in that it allows us to model any type of floor plan and to take into consideration different types of obstacle, such as windows and doors. The algorithm works in a two dimensional environment which simplifies the ray tracing algorithm and reduces the time necessary for the program to run.

In analysing the performance of sector antennas, we assume the receiver is equipped with six-sector directional antennas whose polarisations are vertical. The  $i$ th antenna pattern is defined by the function

$$g_i(\phi_k) = \begin{cases} f\left(\phi_k - \frac{\pi i}{3}\right) & \text{if } \frac{\pi i}{3} - \frac{\theta}{2} \leq \phi_k < \frac{\pi i}{3} + \frac{\theta}{2} \\ 0 & \text{otherwise} \end{cases} \quad (1)$$

where  $g_i(\phi_k)$  is the normalised power gain and  $\phi_k$  is the orientation angle,  $f(\cdot)$  is assumed to be a sinc function and  $\theta$  is the span of the antenna pattern. If we transmit a narrow pulse

$p(t)$ , the complex envelope of the received signal in the  $i$ th is given by

$$h_i(t) = \sum_{k=0}^n \beta_k e^{-j\theta_k} p(t - \tau_k) g_A(\phi_k) \quad (2)$$

where  $\beta_k$ ,  $\theta_k$ ,  $\tau_k$  and  $\phi_k$  are determined by the ray tracing algorithm. The impulse response  $h(t)$  for an omnidirectional antenna is obtained from eqn. 2 when  $g_A(\phi_k)$  is set to 1.

**Results and discussions:** Using the ray tracing algorithm a complex indoor environment was simulated. For the analysis of the performance of BPSK and BPSK/DFE modems for a given  $h_i(t)$  or  $h(t)$ , the method described in Reference 5 and the carrier and timing recovery methods analysed in References 6 and 7 are used.

The transmitter power is 100 mW and the carrier frequency is 18 GHz. The background noise level is determined from  $kTB$  where  $k$  is the Boltzmann constant,  $B$  is the received bandwidth and  $T$  is the temperature of the room. The received front end noise is assumed to be 9 dB. The received attenuation at 1 m from the transmitter which depends on the received antenna characteristics is assumed to be 40 dB. To calculate the outage probability, the probability of error for each location of the transmitter is calculated and is compared with the threshold of  $10^{-5}$ .

We have chosen to simulate one part of the Atwater Kent Laboratories at Worcester Polytechnic Institute, Worcester, MA that includes seven different rooms (Fig. 1). The transmitter is located at the centre of room 1 and the receiver is moved to different locations in the floor plan. The maximum data rates for four different kinds of modem in each room and for the entire floor plan are obtained.

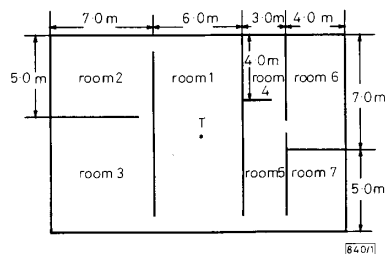


Fig. 1 Floor plan of one part of Atwater Kent Laboratories

From Table 1, it can be seen that the average maximum data rate over the entire floor plan is 15 Mbit/s for a BPSK/DFE modem with omnidirectional antennas and 12 Mbit/s for a BPSK modem with sector antennas. The DFEs with three forward taps and three feedback taps are slightly better than the six-sector antennas. In the small LOS environment, such as room 1, high data rates can be achieved using each technique. If the receiver moves to one of the adjoining rooms,

Table 1 MAXIMUM DATA RATES FOR DIFFERENT MODEMS IN DIFFERENT ROOMS

Room	Maximum data rate (Mbit/s)			
	Omnidirectional	DFE	Sector	Sector + DFE
1	8	40	50	50
2	4	15	13	20
3	5	20	12	25
4	4	20	20	40
5	7	25	30	50
6	2	6	8	12
7	2	7	8	15
Overall	5	15	12	20

The criterion is that if the error rate threshold is  $10^{-5}$ , the acceptable outage rate is assumed to be less than 0.01

such as rooms 2-5, the BPSK/DFE modem with omnidirectional antennas can still attain a data rate of above 15 Mbit/s. However, the maximum data rate for the BPSK modem with the sector antennas in room 2 drops to 12 Mbit/s. In rooms 6 and 7, only the BPSK/DFE with sector antennas can achieve a data rate of above 10 Mbit/s and sector antennas are slightly better than DFEs.

The worst performance is achieved in room 6. Fig. 2 shows that if the data rate is below 12 Mbit/s, the performance of the BPSK modem with sector antennas is better than a BPSK/DFE modem with omnidirectional antennas. However, the sector antenna seems to be less effective for a data rate higher than 15 Mbit/s in this worst case.

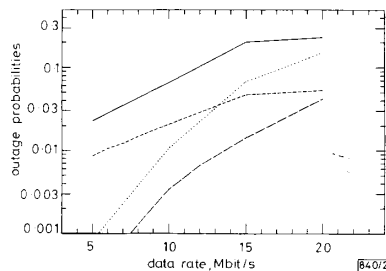


Fig. 2 Outage probabilities against data rates for four kinds of modem in room 6

— omnidirectional  
 ..... sector  
 - - - - DFE  
 - · - · - sector + DFE

**Conclusions:** The deterministic model provides more information than a statistical model because it can provide the direction of the paths and can account for variations in room layout and the materials in the design. Using this model, the comparative performance evaluation of BPSK and BPSK/DFE radio modems with omnidirectional and six-sector antennas was given in a practical environment. In this environment the layout of the rooms and the floor plan has a significant effect on the performance of the different modems. It was shown that in a line-of-sight (LOS) environment, a six-sector antenna is more effective than the DFE with an omnidirectional antenna. For an obstructed-line-of-sight (OLOS) environment the DFE is more effective than the six-sector antenna at eliminating the effects of multipath. Over all the areas examined, a BPSK/DFE modem with sector antenna can provide data rates of the order of 20 Mbit/s.

**Acknowledgments:** The authors would like to thank J.-F. Lee for his help with the ray tracing algorithm.

24th April 1992

G. Yang, K. Pahlavan and T. Holt (Center for Wireless Information Network Studies, Department of Electrical Engineering, Worcester Polytechnic Institute, Worcester MA 01609, USA)

References

- 1 FREEBURG, T. A.: 'Enabling technologies for wireless in-building network communications—four technical challenges, four solutions', *IEEE Communications Magazine*, April 1991, pp. 58-64
- 2 HOWARD, S., and PAHLAVAN, K.: 'Performance of a DFE modem evaluated from measured indoor radio multipath profiles'. Proc. IEEE ICC, Atlanta, GA, June 1990, pp. 1341-1345
- 3 DESCHAMPS, G. A.: 'Ray techniques in electromagnetics', *Proc. IEEE*, September 1972, 60, (9), pp. 1022-1035
- 4 LAWTON, M. C., DAVIES, R. L., and MCGEEHAN, J. P.: 'A ray launching method for the prediction of indoor radio channel characteristics'. IEEE Int. Symp. on Personal, Indoor and Mobile Radio Communications, King's College London (UK), September 1991, pp. 104-108
- 5 PAHLAVAN, K.: 'Comparison between the performance of QPSK, SQPSK, QPR, and SQPR systems over microwave LOS channels', *IEEE Trans.*, March 1985, COM-33, pp. 291-296

- 6 VALENZUELA, R. A.: 'Performance of quadrature amplitude modulation for indoor radio communications', *IEEE Trans.*, November 1987, COM-35, pp. 1236-1238
- 7 GREENSTEIN, L. J., and CZEKAJ-AUGUN, B. A.: 'Performance comparisons among digital radio techniques subjected to multipath fading', *IEEE Trans.*, May 1982, COM-30, pp. 1184-1197

## MIXED INTEGER PROGRAMMING METHOD FOR FAULT DIAGNOSIS OF LINEAR ANALOGUE CIRCUITS

V. C. Prasad, S. N. R. Pinjala and K. G. Murty

*Indexing terms:* Fault diagnosis, Analogue circuits, Mathematical techniques

Fault diagnosis of linear analogue circuits can be formulated as a mixed integer programming problem. This avoids testing all possible combinations of submatrices of the equations of the network to determine faults.

**Introduction:** There are broadly two approaches for analogue fault diagnosis [1, 4, 5]. They are the fault analysis approach or simulation-after-test, and the fault dictionary approach or simulation-before-test. In this Letter, we are concerned with the first approach. In one kind of fault analysis approach called fault verification, equations of the nominal network are obtained. If  $k$  or less elements or nodes are faulty (a node is said to be faulty if at least one of the elements connected to it is faulty), then all submatrices of order  $k$  and above of the equations of the network are to be tested for singularity. From this information, faults can be identified. In general, this is time consuming as all possible submatrices have to be tested. Moreover, this is a brute force method. We formulate it as a 0-1 mixed integer programming problem which can be solved efficiently in a systematic way.

**Mixed integer programming formulation:** Let  $N$  be any linear analogue network which has to be analysed for faults. Extract all independent sources and all pairs of nodes at which voltage measurements are made as ports. Let these be  $m$  ports. Create one port across each of the  $n$  elements to be tested for faults. The equations of such a multiport network using short circuit admittances can be decomposed into two matrix equations of the form

$$Y_{11} V^m + Y_{12} V^n = I^m \quad (1)$$

$$Y_{21} V^m + Y_{22} V^n = I^n \quad (2)$$

where  $I^m(V^m)$  are vectors of currents (voltages) of the ports corresponding to independent sources and measurement ports. Similarly,  $I^n$  and  $V^n$  refer to the set of ports created across the elements which are likely to be faulty. The  $y$  parameters are for the nonfaulty network. Note that  $I^n = 0$ . When a fault occurs, an admittance  $y$  changes to  $y + \Delta y$ . This change  $\Delta y$  is shown as an external connection at the port of the faulty element. With this interpretation,  $I^n$  for the faulty network ( $\bar{I}^n$ ) is nonzero. In fact

$$\bar{I}^n = -\Delta Y_n \bar{V}^n \quad (3)$$

and

$$\Delta I^n = \bar{I}^n - I^n$$

where  $\bar{V}^n$ ,  $\bar{I}^n$ ,  $\bar{I}^m$  refer to the port voltages and currents of the faulty network. If our interest is in node fault diagnosis, ports will have a common node called the reference node and  $\Delta I^n$  is interpreted as changes in the nodal currents due to faults [1].

Let

$$\Delta V^m = \bar{V}^m - V^m \quad \Delta V^n = \bar{V}^n - V^n \quad \bar{I}^m = I^m$$

Therefore, the equations of the faulty network are

$$Y_{11} \bar{V}^m + Y_{12} \bar{V}^n = I^m \quad (4)$$

$$Y_{21} \bar{V}^m + Y_{22} \bar{V}^n = \bar{I}^n \quad (5)$$

From eqns. 1 and 4, we have

$$Y_{11} \Delta V^m + Y_{12} \Delta V^n = 0 \quad (6)$$

From eqns. 2 and 5, we have

$$Y_{21} \Delta V^m + Y_{22} \Delta V^n = \Delta I^n \quad (7)$$

Using eqn. 7, solve for  $\Delta V^n$  and substitute in eqn. 6. This gives an equation of the form

$$Y_m \Delta V^m = Y_n \Delta I^n \quad (8)$$

Inverting the coefficient matrix of  $\Delta V^m$ , we obtain an equation of the form

$$\Delta V^m = Z \Delta I^n \quad (9)$$

where  $Z$  is a rectangular matrix of order  $m \times n$ . This type of equation arises in many fault verification procedures [1, 4]. Eqns. 8 or 9 can be used to determine  $\Delta I^n$  and hence to identify the faults. However, they cannot be solved as they are because there are only  $m$  equations in  $n$  unknowns. Let  $k$  elements be faulty ( $k \leq m-1$ ). Choose  $(n-k)$  components of  $\Delta I^n$  as zero and solve for the remaining components of  $\Delta I^n$  using eqn. 9. There are  ${}^nC_k$  possible sets of such equations. All fault verification procedures assume that only one of these sets gives consistent equations to determine the fault uniquely [1, 5]. (The reader is referred to the literature for more details on this.) We can avoid checking  ${}^nC_k$  possible sets by formulating it as a 0-1 mixed integer programming problem as shown below.

Let

$$\Delta I \triangleq \Delta I^n = [\Delta I_1 \quad \Delta I_2 \quad \dots \quad \Delta I_n]^T$$

and

$$\Delta V \triangleq \Delta V^m = [\Delta V_1 \quad \Delta V_2 \quad \dots \quad \Delta V_m]^T$$

where the superscripts are deleted for simplicity of notation.

Let  $\alpha$  be a large positive number such that the magnitude of every component of  $\Delta I$  is less than  $\alpha$ ; then  $-\alpha x_j \leq \Delta I_j \leq \alpha x_j$  and  $x_j = 0$  or 1 for all  $j = 1, 2, \dots, n$ , i.e.

$$2\alpha x_j - y_j \geq 0 \quad \text{and} \quad y_j \geq 0$$

where

$$y_j = \Delta I_j + \alpha x_j \quad \text{for all } j = 1, 2, \dots, n \quad (10)$$

Thus eqn. 9 can be written as

$$\begin{aligned} Zy - \alpha Zx &= \Delta V \\ y \geq 0 \quad 2\alpha x - y &\geq 0 \quad x_j = 0 \text{ or } 1 \\ &\text{for all } j = 1, 2, \dots, n \quad (11) \end{aligned}$$

$\sum_{j=1}^n x_j$  has a minimum value at the solution when  $x_j$  is allowed to take only two values 0 or 1. Therefore, solving eqn. 9 is equivalent to solving the following 0-1 mixed integer programming (IP) problem:

$$\left[ \begin{array}{l} \text{Minimise } \sum_{j=1}^n x_j \text{ subject to} \\ Zy - \alpha Zx = \Delta V \quad y \geq 0 \quad 2\alpha x - y \geq 0 \\ x \geq 0 \quad \text{and } x_j = 0 \text{ or } 1 \\ \text{for all } j = 1, 2, \dots, n \quad (12) \end{array} \right] \quad (A)$$

Once this problem is solved, the value of  $\Delta I$  can be computed using eqn. 10.